

# Stabilization of Neutral Polyfluorene in Aqueous Solution through Their Interaction with Phospholipids and Sol–Gel Encapsulation

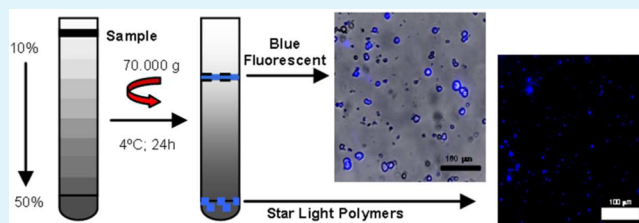
Ricardo Mallavia,\* Maria José Martínez-Tomé, Rebeca Vázquez-Guilló, Zehra Kahveci, Amparo Estepa, and C. Reyes Mateo

Instituto de Biología Molecular y Celular, Universidad Miguel Hernández de Elche, Edificio Torregaitán. Avda. de la Universidad s/n, Alicante 03202, Elche, Spain

## Supporting Information

**ABSTRACT:** Interaction between poly[9,9-bis(6'-bromohexyl)-2,7-fluorene-co-alt-1,4-phenylene] (PFPBr<sub>2</sub>), a neutral conjugated polyfluorene which is completely insoluble in water, and zwitterionic phospholipids has been investigated in order to generate new fluorescent structures which are stable in aqueous media as a means of extending the biological applications of these kinds of polymers. Two types of differently shaped and composed fluorescent structures were identified and then isolated and characterized separately using different biophysical techniques. The first structure type, corresponding to liposomal complexes, showed a fluorescence band centered around 405 nm and maximum absorption at 345 nm, while the second, corresponding to polymer–phospholipid aggregates of variable sizes with lower lipid content, absorbed at longer wavelengths and displayed a well resolved fluorescence spectrum with a maximum centered at 424 nm. Both structures were stable in a large range of pH, and their fluorescence intensity remained practically unaltered for 10 days; it then began to decrease, which was probably because of aggregation. Encapsulation of these structures within the pores of a sol–gel matrix did not affect their fluorescent properties but increased their stability, avoiding further aggregation and subsequent precipitation.

**KEYWORDS:** polyfluorene, phospholipid, liposomes, sol–gel matrix, stabilization, encapsulation



## INTRODUCTION

Conjugated polymers (CPs) are probably among the organic materials with the broadest range of applications, for example, from antistatic coatings, electrodes, and transistors to light-emitting diodes, large area displays, photodetectors, photovoltaic cells, and lasers, etc.<sup>1–6</sup> This versatility is mainly related to the fact that this material can switch from a nonemitting state to a fluorescent state in response to small environmental changes. Consequently, CPs have the necessary properties to be considered a promising new class of sensory materials.<sup>7–9</sup> In this sense, fluorene-based CPs and copolymers are good alternatives to conventional CPs for sensor applications, because they have combined high sensitivity and selectivity and provide a higher response in blue fluorescence reducing interferences generated by other compounds.<sup>10,11</sup> Despite their excellent photophysical and electrochemical properties, the use of fluorene-based CPs for designing new sensors with applicability to biological samples<sup>12</sup> or direct diagnostic tests is made difficult by their low solubility and quantum yield in an aqueous environment. A common strategy applied to increase the aqueous solubility of polyfluorenes is based on the enhancement of the macromolecule polarity, by appending hydrophilic side chains to the main polymer chain.<sup>13–17</sup> Alternative strategies may include encapsulating the backbone of the polyfluorene with suitable macrocycles<sup>18</sup> and/or its interaction with surfactants.<sup>19,20</sup>

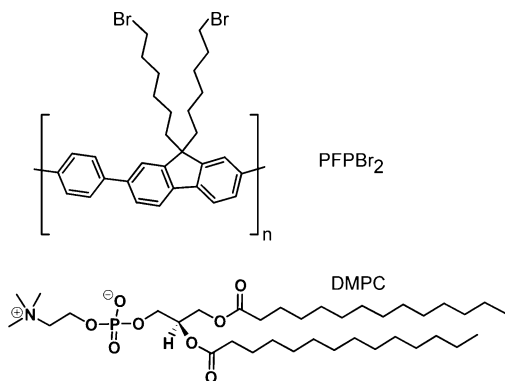
Synthetic phospholipids have good surfactant properties, such as low toxicity and quick biodegradation, and they have also been commercially available in a high state of purity.<sup>20,21</sup> In contact with water and under appropriate conditions, they can form cellular structures known as liposomes, which are able to solubilize a wide variety of nonpolar compounds. The inclusion of polymers in liposomes has been studied as a way to increase the long-term stability of the liposomes, increasing their applications as drug delivery carriers.<sup>22</sup> For this reason, phospholipids could be considered as ideal candidates to interact with nonpolar polyfluorenes so as to form fluorescent complexes which are stable in aqueous environments. The existence of interactions between phospholipids and neutral polyfluorenes has recently been reported by our group<sup>23</sup> and by Tapia et al.<sup>24</sup>

This study aims to gain further insight into the complexes formed, by using the blue light emitting neutral conjugated polymer, PFPBr<sub>2</sub> (poly[9,9-bis(6'-bromohexyl)-2,7-fluorene-co-alt-1,4-phenylene]), and the zwitterionic phospholipid, DMPC (1,2-dimyristoyl-*sn*-glycerol-3-phosphocholine), as a model (Chart 1). By combining different experimental techniques, upon interaction between PFPBr<sub>2</sub> and DMPC, two types of

Received: July 30, 2012

Accepted: March 29, 2013

Published: March 29, 2013

Chart 1. Chemical Structure of PFPBr<sub>2</sub> and DMPC

fluorescent structures were identified, which were isolated and characterized separately. Both structures were found to have different composition and fluorescent properties and were stable in aqueous media in a large range of pH values. The long-term stability of the complexes formed was improved after their encapsulation within the pores of a sol–gel glass, which also permitted easy manipulation of the material and extended their potential biomedical applications in the development of biological chemical sensors and drug delivery platforms.

## MATERIAL AND METHODS

**Reagents.** All materials used for buffer and gradient preparations—sodium phosphate, Tris–HCl, Tris base sucrose, and 2-dimyristoyl-*sn*-glycerol-3-phosphocholine (DMPC)—were purchased from Sigma-Aldrich Chemical Co., St. Louis, MO. Neutral conjugated poly[9,9-bis(6'-bromo-hexyl)-2,7-fluorene-*co-alt*-1,4-phenylene], (PFPBr<sub>2</sub>), was synthesized and characterized as previously described ( $M_w = 10.0 \text{ kg}\cdot\text{mol}^{-1}$ ; PDI = 2.0; DP = 17 based on polyfluorene calibration).<sup>25,26</sup>

**Preparation of DMPC Vesicles.** A stock solution of DMPC was prepared in chloroform, in the absence or presence of PFPBr<sub>2</sub>, at an adequate polymer-to-lipid molar ratio (1:5).<sup>23</sup> Chloroform solutions were then dried under a stream of argon to obtain a thin film at the bottom of a small thick-walled glass tube. After removing the traces of organic solvent, the film was resuspended in sodium phosphate buffer (10 mM, pH 7.4) to reach a final lipid concentration of 0.5 mM. The suspension was then heated at 40 °C and vortexed for 30 min. This method yields multilayer lipid vesicles (MLVs), with typical diameters between 0.5 and 1  $\mu\text{m}$ .

**Isolation of PFPBr<sub>2</sub>-DMPC complexes.** Sucrose gradient centrifugation was used to isolate the PFPBr<sub>2</sub>-DMPC complexes following the previously described procedures.<sup>27,28</sup> The DMPC vesicles (prepared in the absence or presence of PFPBr<sub>2</sub>) were layered onto a 10–50% discontinuous sucrose gradient created by gently overlaying lower concentrations of sucrose with higher concentrations in a centrifuge tube. In this case, the sucrose gradient consists of nine sucrose fractions of 1 mL extending from 10 to 50% sucrose in 5% increments. Sucrose solutions were prepared in Milli-Q water.

The gradient was then centrifuged for 24 h in a Beckman SW 41 rotor at 70,000 g and 4 °C. After centrifugation, each sucrose layer (1 mL) was removed sequentially from the top of the gradient using a different sterile pipet for each layer and fluorescent bands or fractions visible under UV light were washed twice with Milli-Q water, lyophilized, and kept at 4 °C until use.

**Immobilization in Sol–Gel Matrix.** Silica stock solution was prepared by mixing 4.46 mL of TEOS, 1.44 mL of water (Milli-Q), and 0.04 mL of 0.6 M HCl in a closed vessel. The mixture was stirred for 1 h, and alcohol was subsequently removed by means of rotaevaporation. Afterward, 700  $\mu\text{L}$  of the PFPBr<sub>2</sub>/DMPC complexes was mixed with 700  $\mu\text{L}$  of deoxygenated silica stock solution in a

disposable polymethylmethacrylate cuvette. Gelation readily occurred after mixing. After 1 h, monoliths, of  $\sim 9 \times 9 \times 12 \text{ mm}^3$ , were washed three times with phosphate buffer and were wet aged in 0.5 mL of the same buffer at 4 °C for 24 h. Cuvettes were covered with parafilm and stored in the dark at 4 °C before use.

**pH and Time Stability Assays.** About 20  $\mu\text{L}$  from samples washed in Milli-Q water was added to 1.5 mL of a different buffer solution freshly prepared from Tris–HCl and Tris-base (10 mM both), with pH values ranging between 2.5 and 13.5. Stability was assessed by monitoring the fluorescence spectra of the complexes at the different pHs and plotting their area in relation to that obtained at pH 7.5. Samples at pH 7.5 and at room temperature were selected for the time stability assays.

**Instrumentation. Microscopy.** Inverted fluorescence or epifluorescence microscopy was carried out using a Nikon Eclipse TE2000-U inverted microscope equipped with a Nikon Digital Sight DS-1QM/H and Nikon Digital Camera DXM1200C. We used a homemade stainless-steel chamber where approximately 500  $\mu\text{L}$  of preparation was deposited over a glass surface. Data acquisition was monitored successively by manual format, and data were processed using NIS-Elements AR 2.30 software. Transmission electron micrographs (TEM) were performed using a Jeol 1010 microscope (Jeol, Japan), operating at 80,000 kV. Samples were prepared by placing a drop of the sample onto a 400-mesh copper grid coated with carbon film, and after staining with uranyl acetate, they were left to air-dry before being placed under the microscope. Images were recorded with a Megavideo III camera. Acquisition was accomplished with the Soft-Imaging software (SII, Germany).

**Spectroscopy.** Fluorescence and steady-state anisotropy measurements were performed at room temperature in a PTI-QuantaMaster spectrofluorometer, with automatically controlled Glan-Thompson polarizers. Data acquisition was processed with Felix32 software. Samples containing the fluorescent complexes (buffer suspensions and sol–gel monoliths) were placed in  $10 \times 10 \text{ mm}^2$  path length quartz cuvettes, and fluorescence emission spectra were recorded between 390 and 570 nm. Background intensities were always checked and subtracted from the sample when necessary. Experiments were repeated at least twice.

Proton nuclear magnetic resonance (<sup>1</sup>H NMR) experiments were performed on a Bruker AVANCE 500 MHz spectrometer. The <sup>1</sup>H NMR spectra were collected at 296 K in deuterated chloroform at 0.03% in TMS as an internal reference. Estimation of the integrated area for the molar ratio between components (DMPC and PFPBr<sub>2</sub>) was carried out using identical gain, scans, and relaxation delay relation.

**Calorimetry.** Differential scanning calorimetry was performed using a purged N<sub>2</sub>(g) atmosphere at a heating/cooling rate in a Perkin-Elmer Pyris model 6 apparatus. Data acquisition was monitored with Pyris manager software, and processing was carried out using Origin 7.0 software. Differences in heat capacity between the samples and the reference, which contained only liposomes, were obtained at a heating rate of 1.50 °C/min. Samples and reference were scanned from –2.0 up to 45.0 °C. A series of three consecutive scans of the same sample was made to ensure scan-to-scan reproducibility and average.

## RESULTS AND DISCUSSION

**Detection and Isolation of Fluorescent PFPBr<sub>2</sub>-DMPC Complexes.** Poly[9,9-bis(6'-bromohexyl)-2,7-fluorene-*co-alt*-1,4-phenylene] (PFPBr<sub>2</sub>) is a neutral conjugated polymer with an interesting synthetic projection, as a precursor of polyelectrolytes and naturally for its luminescent properties,<sup>9</sup> but completely insoluble in water and therefore nonfluorescent in this medium.<sup>29</sup> This fact, common in many polyfluorenes, reduces their potential applications in environmental and biomedical sectors. Given the hydrophobic nature of PFPBr<sub>2</sub>, to improve solubility, we explored their possible incorporation into liposomes composed of the zwitterionic lipid DMPC. As a preliminary experiment, aliquots of PFPBr<sub>2</sub> in chloroform were

added to an aqueous suspension of DMPC liposomes, which were well above their transition temperature (23 °C), but no fluorescent signal was observed. This result indicates that PFPBr<sub>2</sub> does not spontaneously interact with liposomes, probably because the polymer readily aggregates once in the aqueous media, and precipitates before its union with liposomes can take place.

Previous experiments performed in our laboratory showed that the interaction between PFPBr<sub>2</sub> and liposomes can be favored by simultaneously dissolving the polymer in chloroform with the phospholipids, before forming the liposomes, as described in the Materials and Methods.<sup>23</sup> Following this protocol, we mixed chloroform solutions of both compounds at a molar ratio of 5:1 (DMPC:PFPBr<sub>2</sub>). The sample was dried under a vacuum and the solid film resuspended in buffer and placed in a fluorescent cuvette. The interaction between PFPBr<sub>2</sub> and phospholipid was made evident by the appearance of a fluorescence band with a peak of around 425 nm upon excitation at 370 nm (Figure 1), which was almost similar in

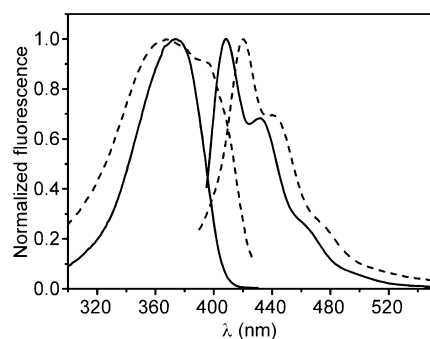


**Figure 1.** Normalized fluorescence excitation (left) and emission spectra (right) of PFPBr<sub>2</sub> in chloroform (full line) and DMPC (dashed line), recorded fixing the wavelengths at 445 and 370 nm, respectively.

shape to the one corresponding to PFPBr<sub>2</sub> in chloroform (maximum emission at 408 nm), with a lower resolution and shifted to red. Figure 1 also shows the fluorescence excitation spectrum of the sample obtained at 445 nm. In this case, the band was clearly broader than the one recorded in organic solvent with the appearance of a shoulder around 490 nm. The increase of the spectral width in the fluorescence excitation spectrum suggests emission from different polymer populations. To further explore this hypothesis, the sample was excited at different wavelengths and the emission spectra were compared in the same region (Figure 2A). Results show that the shape of the spectrum depends on the excitation wavelength, indicating that there are at least two polymer populations with different fluorescent properties, one emitting around 400 nm and the other with maximum emission at 425 nm. When the excitation spectra were recorded with the emission wavelength fixed at 390, 445, and 475 nm (Figure 2B), two different spectra were observed, which supports the existence of these two populations. This fact led us to work on the separation and characterization of these components using different approaches.

First, we evaluated the different populations, according to their density, using discontinuous sucrose density gradient ultracentrifugation, because it is often used to purify enveloped biological membranous structures.<sup>27,28</sup> Samples were placed onto a sucrose gradient, which was centrifuged for 1 day below room temperature to preserve the vesicle structure. Following

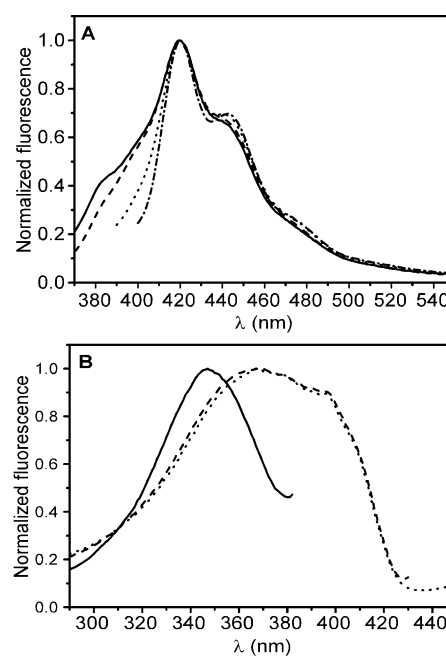
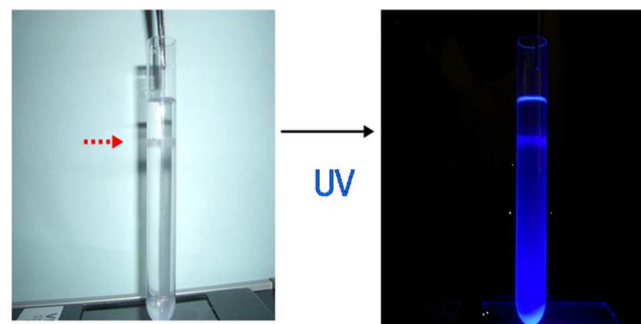


Figure 2

**Figure 2.** (A) Fluorescence emission spectra of PFPBr<sub>2</sub> in DMPC upon excitation at 330 (full line), 350 (dashed line), 370 (dotted line), and 390 nm (dot-dashed line). (B) Fluorescence excitation spectra of PFPBr<sub>2</sub> in DMPC recorded fixing the emission wavelength at 390 (full line), 445 (dashed line), and 475 nm (dotted line).

this operation, two major bands appeared with high fluorescent response under ultraviolet light: the narrow one corresponded to 1.07 g·cm<sup>-3</sup> (15–20% sucrose; *top fraction* denoted as TF), and the broader one was 1.2 g·cm<sup>-3</sup> (45–50% sucrose; *bottom fraction* denoted as BF) (Figure 3). Bands were recovered from the gradient after being nonquantitatively collected with a syringe, placed in different vials, and washed twice with Milli-Q water.



**Figure 3.** Methodology and identification of the fluorescent fractions, once isolated using discontinuous sucrose gradient ultracentrifugation.

**Characterization of PFPBr<sub>2</sub>–DMPC Complexes.** The appearance of two major fluorescent bands in the sucrose gradient supports the previously postulated existence of two different polymer populations resulting from the interaction with DMPC. Fluorescence properties of both populations (TF and BF) were explored by recording their fluorescence spectra (Figure 4). The excitation and emission bands from TF showed low resolution, with intensity maxima at 345 and 405 nm, respectively.

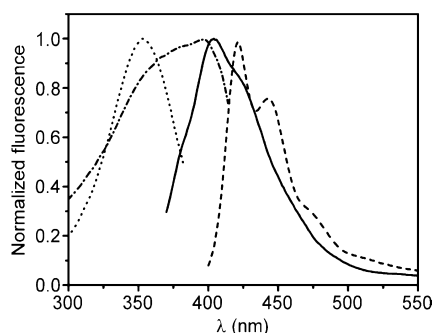


**Figure 4.** Excitation and emission spectra corresponding to top and bottom fractions in water solution. The emission spectrum of TF was recorded upon excitation at 340 nm (full line), the excitation spectrum of TF fixing the emission wavelength at 400 nm (dotted line), the emission spectrum of BF exciting at 370 nm (dashed line), and the excitation spectrum of BF fixing the emission wavelength at 422 nm (dot-dashed line).

In contrast, fluorescence spectra corresponding to BF were red-shifted and the emission spectrum showed a higher resolution in the vibrational structure, with two peaks at 425 and 445 nm. A similar emission spectrum has recently been reported for the interaction of the cationic derivative polyfluorene HTMA–PFP with surfactants or proteins in water.<sup>24,30</sup> The shape and position of the absorption and emission spectrum of conjugated polyfluorenes are known to be related to the degree of polymer aggregation.<sup>30,31</sup> Because of the hydrophobic backbones of polyfluorenes, they have a high tendency to aggregate in an aqueous environment, which leads to red spectral shift of the absorption and emission maxima. In addition, aggregation reduces the number of degrees of the polymer chain's freedom and hence decreases in the number of conformations present in the excited state. Therefore, our results suggest that PFPBr<sub>2</sub> in TF should be in a non-aggregate state, as isolated polymer chains interacting with DMPC, while in BF polymer chains and lipids should be aggregated.

We have characterized these structures more accurately by analyzing the fluorescence depolarization of the samples. Measurements of steady-state anisotropy were performed in bottom and top fractions at room temperature, and details are presented in the Supporting Information. Figure S2 (Supporting Information) shows comparative experimental results obtained for this polyfluorene in different media. The value of anisotropy in TF was high,  $r = 0.22 \pm 0.02$ , not very far from the value corresponding to the intrinsic anisotropy of the polymer<sup>32</sup> and close to the value obtained in chloroform solution ( $r = 0.19 \pm 0.02$ ).<sup>33</sup> In contrast, in BF, fluorescence is highly depolarized with  $r = 0.04 \pm 0.02$ , as occurs in solid state  $r = 0.08 \pm 0.02$ .<sup>32</sup> Therefore, taking into account that fluorescence depolarization in polyfluorenes is mainly caused by energy transfer between adjacent polymer chains, and not by the rotational motion of the excited fluorophore, we consider that these results support the above hypothesis regarding the composition of both fractions: in TF, the polymer chains should be isolated in layers of phospholipids reducing the energy transfer depolarization process and acting as a good solvent, while BF should be constituted by aggregates of nonordered polymers.

To visualize both populations, samples were observed under fluorescence microscopy. Figure 5A shows the overlapped images corresponding to TF, obtained upon irradiation with

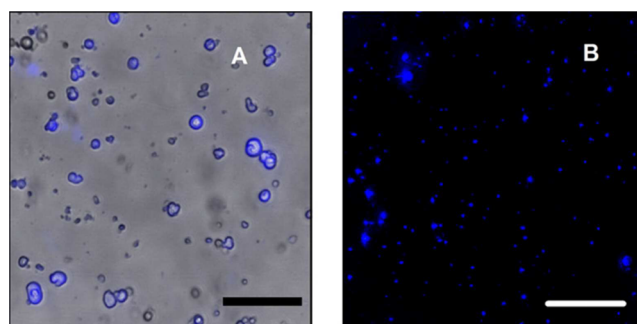


**Figure 5.** Fluorescence microscopy images obtained for top (A) and bottom fractions (B). Scale bar corresponding to 100  $\mu\text{m}$ .

UV and visible light. Spherical liposomes, displaying a blue fluorescence, were clearly observed, which suggested that the polymer is grafted onto the lipid bilayer. These images are different from those corresponding to BF under UV light (Figure 5B), which showed blue fluorescent particles of heterogeneous shape and size. To get more insight into the size and shape of these structures, transmission electron microscopy (TEM) analysis was performed using a negative stained protocol for biological samples, as described in the Materials and Methods. Images corresponding to both structures are shown in Figure 6A and B and compared to those obtained from liposomes (MLVs) of pure DMPC which were fabricated in the absence of PFPBr<sub>2</sub> and isolated in the same percentage of sucrose (Figure 6C). Results show that the structures corresponding to TF are spherical with a diameter of around 500–800 nm and similar to those observed in the absence of polymer, while those corresponding to BF present variable size clusters. The dry mass of each fraction was approximately  $60 \pm 5\%$  (TF: 15–20%) and  $25 \pm 5\%$  (BF: 45–50%) in relation to the initial sample. We also made a rough estimation based on the composition of these structures from <sup>1</sup>H NMR experiments. Comparative spectra confirmed the presence of DMPC and PFPBr<sub>2</sub> in both fractions with different ratios (see details in the Supporting Information). Estimation was made from the integration area of the methylene protons in the polymer chain with respect to the protons in the methyl groups of the myristoyl chains. Results showed molar ratios of DMPC with respect to unity of the polymer PFPBr<sub>2</sub> (DP = 17 based on polyfluorene calibration) of around 280:1 and 11:1 for the top and bottom fluorescent fractions, respectively.

Finally, to confirm the existence of liposomes exclusively in TF, we performed DSC experiments on the samples collected from TF and BF bands and also on the samples containing liposomes (MLVs) of DMPC, which were prepared in the absence of polymer. Liposomes of pure DMPC are known to show two endothermic peaks at about 14 and 23 °C, corresponding to a less energetic pretransition and a more energetic main transition, respectively. Both transitions are very cooperative and characterized by sharp peaks in the thermal scans. Figure 7 shows the DSC thermograms for the samples corresponding to TF, BF, and polymer free liposomes. The position, height, and width of the main peaks were almost similar for TF and pure liposomes, indicating that the cooperativity of the transition is not altered in the presence of PFPBr<sub>2</sub> and that the polymer does not disrupt the integrity of the liposomes. There are probably not many polymer chains in the lipid bilayer, which is supported by the fact that the density of liposomes is similar in the absence and presence of

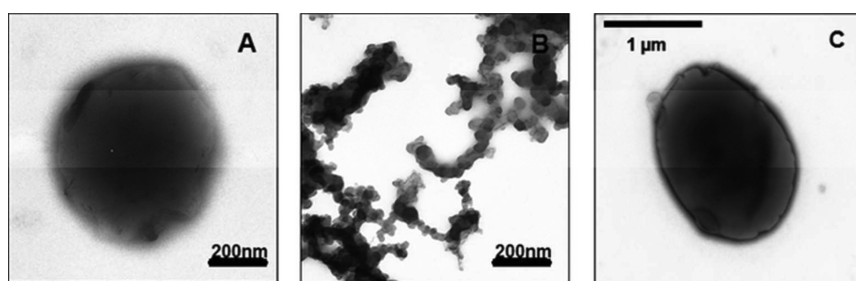


**Figure 6.** Transmission electron micrographs, negatively stained in isolated fractions: Top (A) and bottom (B) fractions. Control of MLV's isolated at 20% sucrose in the same procedure (C).

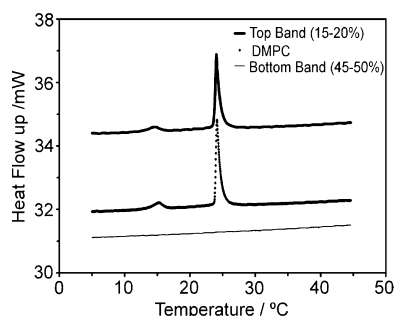


**Figure 7.** DSC thermograms corresponding to TF (thick line), BF (thin line), and MLVs of pure DMPC (points).

PFPBr<sub>2</sub>. In contrast, no transition was observed in the DSC thermogram corresponding to BF, which confirms that phospholipids in the clusters are not arranged in bilayers to form liposomes.

From the above results, it is possible to conclude that two different fluorescent structures coexist in aqueous media upon the interaction of PFPBr<sub>2</sub> with zwitterionic phospholipids. One is less dense than the other and is mainly constituted by liposomes of homogeneous size, which contain PFPBr<sub>2</sub> solubilized inside the bilayer as isolated polymer chains. The other should be formed by polymer/phospholipid complexes aggregated in clusters. Note that, besides the two main fluorescent bands detected in the sucrose gradient (see Figure 3), a weak fluorescent signal is observed at intermediate densities whose intensity increases from top to bottom. Fluorescence spectra corresponding to these bands (20–45% sucrose) displayed the same shape as those corresponding to BF but much lower fluorescence intensity (data not shown). This result confirms the existence of clusters of variable sizes, most of which show high density and are therefore located at the bottom of the gradient, while the smaller ones are placed at intermediate densities. These complexes probably consist of polymer which avoid water contact by forming aggregates with each other, and are stabilized through hydrophobic interactions by phospholipids which place their nonpolar tails toward the polymer aggregates and expose their polar heads to the aqueous phase.

**Stability Assays.** Complex stability was explored as a function of pH (from pH 2.5 to pH 13.5) by monitoring the fluorescence spectra of the samples at the different pHs and plotting their area in relation to that obtained at pH 7.5 (Figure 8). Results show that the fluorescence intensities of both polymer populations are practically preserved in a large range of pH's, even in acid media. However, while the fluorescence corresponding to BF was stable at high pH, that of TF showed a decrease of up to pH 12, probably due to the phospholipid

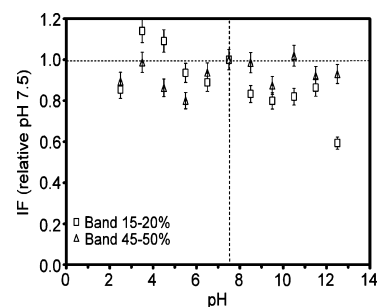


**Figure 8.** Fluorescence intensity (relative to that obtained at pH 7.5) for TF (squares) and BF (triangles) as a function of pH. Dashed lines represent references.

hydrolysis that results from this pH induced membrane breakdown.

Figure 9 shows the stability of the complexes as a function of storage time for samples which were prepared and kept in the

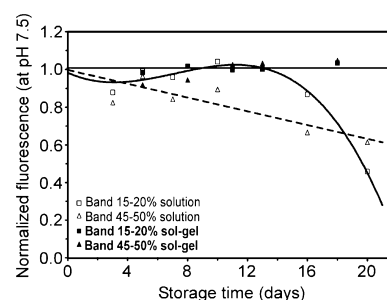


**Figure 9.** Evolution over time of the fluorescence intensity of the different fractions: TF (squares) and BF (triangles) in solution (empty symbols) and immobilized into a sol-gel matrix (filled symbols). Lines represent trends of experimental data.

dark, at 4 °C, for up to 20 days. Stability was evaluated by monitoring the fluorescence spectra of the complexes at room temperature and plotting the area of each spectrum as a function of time (days after preparation). For the first 10 days, small fluctuations of fluorescence intensity were detected for both complexes, but in general, behavior was stable. However, after 10 days, a decrease in fluorescence intensity was observed for both structures, which was probably caused by the aggregation of the complexes and the subsequent precipitation of the aggregates formed.

**Encapsulation of the Complexes in a Sol-Gel Matrix.** Silica sol-gel materials have been shown to be an excellent medium for macromolecule immobilization. Macromolecules are individually caged in the glasses and retained in pores that

protect them from aggregation, providing an environment similar to that of their natural medium. The resulting entrapped macromolecule usually retains its structural integrity and functionality and is accessible to small molecules diffusing into the matrix, all of which enable applications in biosensors and biotechnology.<sup>34–38</sup> Few specific studies on the encapsulation of polyfluorenes in sol–gel matrix were found in the bibliography. In previous research, our group characterized the properties of PFPBr<sub>2</sub>–cyclodextrin complexes as well as the cationic derivative polyfluorene HTMA–PFP complexes after encapsulation in mesoporous silica.<sup>14,29</sup> In addition, Evans et al. have recently demonstrated the macroscale homogeneity of analogue nanocomposite materials in sensor devices.<sup>39</sup>

Taking into account the interesting properties of these materials, the complexes corresponding to TF and BF were separately immobilized in a sol–gel matrix. The excellent optical transparency of the matrix allowed the characterization of both structures within the nanopores through fluorescence spectroscopy. Fluorescence spectra of the immobilized complexes were directly recorded from the sol–gel monolith and are shown normalized in Figure 10. The fact that the emission spectra of the two structures practically coincide with those recorded in solution is indicative of the suitability of the immobilization process.

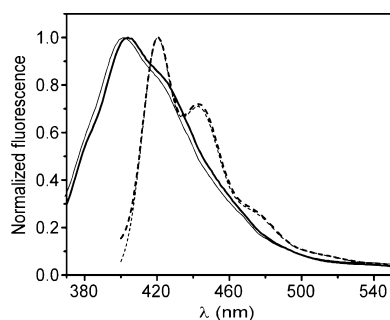


**Figure 10.** Normalized emission spectra corresponding to top (full line) and bottom fractions (dashed line) after sol–gel immobilization (thin lines). Spectra are compared to those obtained for TF and BF in solution (thick lines).

The stability of the immobilized complexes as a function of storage time was explored by monitoring their fluorescence spectra and plotting the area of each spectrum. Results were compared with those obtained from the same complexes before encapsulation (Figure 9). As we can see, the fluorescence intensity was very stable for at least 18 days, in contrast to what occurs in solution. This behavior can be explained because the encapsulation of both polymer populations within the pores of the silica matrix reduces the possibility of aggregation as well as the eventual precipitation of these structures at the bottom of the flask.

## CONCLUSIONS

In this study, the conjugated polymer PFPBr<sub>2</sub>, which is completely insoluble in aqueous media, has been solubilized in a buffer solution through its interaction with zwitterionic phospholipids. This strategy makes it possible to work with neutral CPs in aqueous media, eliminating the need to synthesize new water-soluble CPs. After lipid interaction, two distinct fractions are produced, one of which corresponds to liposomal complexes and the other to polymer–phospholipid

aggregates/clusters. These structures show different composition and specific spectroscopic properties, and both are stable in a large range of pH. In addition, their fluorescence intensity remains practically unaltered for 10 days; afterward, it decreases, probably because of aggregation. The two structures could include small molecular dopants to achieve applications in bioimaging and drug delivery; the use of one or the other will depend on the potential application, taking into account the different polymer aggregation states and fluorescent properties of each fraction. Moreover, these structures can be immobilized in a silica sol–gel glass without their fluorescent properties being affected, leading to considerable increases in their stability, allowing an easy manipulation of the material and extending their potential biomedical applications in the development of conjugated polymer based biosensors.

## ASSOCIATED CONTENT

### Supporting Information

Anisotropy analysis, <sup>1</sup>H NMR mass spectra, and experimental details. This material is available free of charge via the Internet at <http://pubs.acs.org>.

## AUTHOR INFORMATION

### Corresponding Author

\*Phone: 34-966658941. Fax: 34-966658758. E-mail; [r.mallavia@umh.es](mailto:r.mallavia@umh.es).

### Notes

The authors declare no competing financial interest.

## ACKNOWLEDGMENTS

This research was supported by Government sponsored Research Projects MAT-2008-05670, MAT-2011-23007, and PT-2009-002. Finally, we thank Federico J. Paya (FPTAI06-098) for technical assistance and, also, Dr. Alfonso Salinas-Castillo for his help.

## REFERENCES

- (1) Gunes, S.; Neugebauer, H.; Sariciftci, N. S. *Chem. Rev.* **2007**, *107*, 1324–1328.
- (2) Thomas, S. W., III; Joly, G. D.; Swager, T. M. *Chem. Rev.* **2007**, *107*, 1339–1386.
- (3) Hoven, C.; Garcia, A.; Bazan, G. C.; Nguyen, T.-Q. *Adv. Mater.* **2008**, *20*, 3793–3810.
- (4) Scherf, U.; List, E. J. W. *Adv. Mater.* **2002**, *14*, 477–487.
- (5) Grimsdale, A. C.; Chan, H. L.; Martin, R. E.; Jokisz, P. G.; Holmes, A. B. *Chem. Rev.* **2009**, *109*, 897–1091.
- (6) Chocho, C. L.; Choulis, S. A. *Prog. Polym. Sci.* **2011**, *36*, 1326–1414.
- (7) An, L.; Liu, L.; Wang, S. *Asian J. Chem.* **2009**, *4*, 1196–1206 and references therein.
- (8) Tapia, M. J.; Montserin, M.; Valente, A. J. M.; Burrows, H. D.; Mallavia, R. *Adv. Colloid Interface Sci.* **2010**, *158*, 94–107.
- (9) Zhu, C.; Liu, L.; Yang, Q.; Lv, F.; Wang, S. *Chem. Rev.* **2012**, *112*, 4687–4735.
- (10) Jiang, H.; Taranekekar, P.; Reynolds, J. R.; Schanze, K. S. *Angew. Chem., Int. Ed.* **2009**, *48*, 4300–4316.
- (11) Scherf, U.; Neher, D. *Polyfluorenes*; Springer-Verlag: Heidelberg, Germany, 2008; p 274.
- (12) Liu, B.; Bazan, G. C. *J. Am. Chem. Soc.* **2006**, *128*, 1188–1196.
- (13) Huang, F.; Wang, X.; Wang, D.; Yang, W.; Cao, Y. *Polymer* **2005**, *46*, 12010–12015.
- (14) Mallavia, R.; Martinez-Perez, D.; Chmelka, B. F.; Bazan, G. C. *Bol. Soc. Esp. Ceram. Vidrio* **2004**, *43*, 327–330.
- (15) Liu, B.; Gaylord, B. S.; Wang, S.; Bazan, G. C. *J. Am. Chem. Soc.* **2003**, *125*, 6705–6714.

- (16) Chen, Q.; Cui, Y.; Zhang, T. L.; Cao, J.; Han, B. G. *Biomacromolecules* **2010**, *11*, 13–19.
- (17) Burrows, H. D.; Lobo, V. M. M.; Pina, J.; Ramos, M. L.; de Melo, J. S.; Valente, A. J. M.; Tapia, M. J.; Pradhan, S.; Scherf, U. *Macromolecules* **2004**, *37*, 7425–7427.
- (18) Farcas, A.; Jarroux, N.; Harabagiu, V.; Guégan, P. *Eur. Polym. J.* **2009**, *45*, 795–803.
- (19) Tapia, M. J.; Burrows, H. D.; Knaapila, M.; Monkman, A. P.; Arroyo, A.; Pradhan, S.; Scherf, U.; Pinazo, A.; Perez, L.; Moran, C. *Langmuir* **2006**, *22*, 10170–10174.
- (20) Infante, M. R.; Pinazo, A.; Seguer, J. *Colloids Surf., A* **1997**, *123* (124), 49–69.
- (21) Pérez, L.; Infante, M. R.; Angelet, M.; Clapés, P.; Pinazo, A. *Prog. Colloid Polym. Sci.* **2004**, *123*, 210–216.
- (22) Immordino, M. L.; Dosio, F.; Cattel, L. *Int. J. Nanomed.* **2006**, *1*, 297–315.
- (23) Mallavia, R.; Paya, F. J.; Salinas, A.; Estepa, A.; Mateo, C. R. *Proc. SPIE-Int. Soc. Opt. Eng.* **2007**, *6592*, 659213.
- (24) Tapia, M. J.; Monteserin, M.; Burrows, H. D.; Seixas de Melo, J. S.; Pina, J.; Castro, R. A. E.; Garcia, S.; Estelrich, J. *J. Phys. Chem. B* **2011**, *115*, 5794–5800.
- (25) Mallavia, R.; Montilla, F.; Pastor, I.; Velásquez, P.; Arredondo, B.; Alvarez, A. L.; Mateo, C. R. *Macromolecules* **2005**, *38*, 3185–3192.
- (26) Molina, R.; Gómez-Ruiz, S.; Montilla, F.; Salinas-Castillo, A.; Fernandez-Arroyo, S.; Ramos, M.; Micol, V.; Mallavia, R. *Macromolecules* **2009**, *42*, 5471–5477.
- (27) Driessen, A. J.; de Vrij, W.; Konings, W. N. *Proc. Natl. Acad. Sci. U.S.A.* **1985**, *82*, 7555–7559.
- (28) Yamamura, H.; Hayakawa, M.; Imura, Y. *J. Appl. Microbiol.* **2003**, *95*, 677–685.
- (29) Martínez-Tomé, M. J.; Esquembre, R.; Mallavia, R.; Mateo, C. R. *J. Fluoresc.* **2013**, *23*, 171–180.
- (30) Martínez-Tomé, M. J.; Esquembre, R.; Mallavia, R.; Mateo, C. R. *Biomacromolecules* **2011**, *11*, 1494–1501.
- (31) Attar, H. A.; Monkman, A. P. *J. Phys. Chem. B* **2007**, *111*, 12418–12426.
- (32) Montilla, F.; Frutos, L. M.; Mateo, C. R.; Mallavia, R. *J. Phys. Chem. C* **2007**, *11*, 18045–18410.
- (33) Molina, R.; Ramos, M.; Montilla, F.; Mateo, C. R.; Mallavia, R. *Macromolecules* **2007**, *40*, 3042–3048.
- (34) Livage, J.; Coradin, T.; Roux, C. *J. Phys.: Condens. Matter* **2001**, *13*, R673–R691.
- (35) Pastor, I.; Ferrer, M. L.; Lillo, M. P.; Gómez, J.; Mateo, C. R. *J. Phys. Chem. B* **2007**, *111*, 11603–11610.
- (36) Menea, B.; Menea, F.; Aiolfi-Guimaraes, C.; Sharts, O. *Int. J. Nanotechnol.* **2010**, *7*, 1–45.
- (37) Salinas-Castillo, A.; Pastor, I.; Mallavia, R.; Mateo, C. R. *Biosens. Bioelectron.* **2008**, *24*, 1053–1056.
- (38) R. Esquembre, R.; Pinto, S.; Poveda, J. A.; Prieto, M.; Mateo, C. R. *Soft Matter* **2012**, *8*, 408–417.
- (39) Evans, R. C.; Macedo, A. G.; Pradhan, S.; Scherf, U.; Carlos, R. L.; Burrows, H. D. *Adv. Mater.* **2010**, *22*, 3032–3037.